How to cite: *Angew. Chem. Int. Ed.* **2021**, *60*, 21200–21204
International Edition: doi.org/10.1002/anie.202107036
German Edition: doi.org/10.1002/ange.202107036

Photothermal Therapy

Hypoxia-Responsive Gene Editing to Reduce Tumor Thermal Tolerance for Mild-Photothermal Therapy

Xueqing Li[+], Yongchun Pan[+], Chao Chen, Yanfeng Gao, Xinli Liu, Kaiyong Yang, Xiaowei Luan, Dongtao Zhou, Fei Zeng, Xin Han, and Yujun Song**

Abstract: *Near-infrared (NIR)-light-triggered photothermal therapy (PTT) is usually associated with undesirable damage to healthy organs nearby due to the high temperatures (>50 °C) available for tumor ablation. Low-temperature PTT would therefore have tremendous value for clinical application. Here, we construct a hypoxia-responsive gold nanorods (AuNRs)-based nanocomposite of CRISPR-Cas9 for mild-photothermal therapy via tumor-targeted gene editing. AuNRs are modified with azobenzene-4,4′-dicarboxylic acid (p-AZO) to achieve on-demand release of CRISPR-Cas9 using hypoxia-responsive azo bonds. In the hypoxic tumor microenvironment, the azo groups of the hypoxia-activated CRISPR-Cas9 nanosystem based on gold nanorods (APACPs) are selectively reduced by the overexpression of reductases, leading to the release of Cas9 and subsequent gene editing. Owing to the knockout of HSP90α for reducing the thermal resistance of cancer cells, highly effective tumor ablation both in vitro and in vivo was achieved with APACPs under mild PTT.*

The clustered regularly interspaced short palindromic repeats (CRISPR)-associated protein 9 (Cas9) system is composed of the Cas9 nuclease and a single guide RNA (sgRNA).[1] Being an emerging technology in the biological field, CRISPR-Cas9 plays vital roles for gene editing and disease treatment.[2] Up to now, various methods have been developed to deliver CRISPR-Cas9 system, including electroporation,[3] microinjection,[4] viral vectors,[5] and other nonviral vectors.[6] Among the in vivo delivery systems, viral approaches probably trigger unwanted immunogenicity and carcinogenesis.[7] To overcome the biosafety issues, tremendous nonviral strategies have been successfully achieved, but they are still difficult to realize on-demand release of CRISPR-Cas9 that was precisely triggered by disease microenvironment.[8]

Rapid cell proliferation and damaged microvessels at tumor site reduce the oxygen supply by the increased oxygen consumption as well as limited blood supply.[9] The imbalance between insufficient oxygen supply and ever-increasing metabolic demand leads to a typical characteristic of hypoxia in most solid tumor microenvironments.[10] The characteristic promotes more effective platforms to achieve promising cancer treatment strategies. On the one hand, hypoxia enhances the tumorigenesis and resistance to cancer therapy, inspiring extensive researches to fight against it for improvement of the anticancer effect.[11] On the other hand, with the typical characteristic of hypoxia, the tumor-targeted imaging agents and hypoxia-activated prodrugs or carriers have been realized toward precision medicine.[12]

Due to its noninvasive and spatiotemporally controllable mode, photothermal therapy (PTT), a hyperthermia employing light to generate localized heat by specific NIR photoresponse nanomaterials or molecules, has drawn increasing attention in the field of tumor therapy.[13] However, such remedy typically needs a high temperature over 50 °C to ablate tumor, which inevitably causes heating damage to nearby normal tissues and leads to the risk of recurrence or metastasis.[14] Thus, the strategy of mild-temperature PTT to overcome tumor thermoresistance is in urgent need. Existing researches demonstrate that the thermal tolerance at 42–47 °C is associated with a kind of chaperon proteins called heat shock protein (HSP).[15] Among such proteins, HSP90 is overexpressed in tumor cells to maintain homeostasis in harsh microenvironment and promote survival in stress environment.[16] Therefore, inhibition of HSP90α (a major isoform of HSP90) protein provides a potential strategy to achieve a tumor-specific low-temperature hyperthermia in the clinical application.[17]

In this study, we proposed a hypoxia-responsive strategy for targeted delivery of CRISPR-Cas9 system to further realize mild hyperthermia. At normal oxygen partial pressure, the CRISPR-Cas9 system was covalently crosslinked on Au nanorods by a hypoxia-responsive azobenzene linker, azobenzene-4,4′-dicarboxylic acid (*p*-AZO). As the imbalance of cellular redox states in the hypoxic microenvironment of tumor cells contributed to an increase in reducing stress,[18] N-N double bond of *p*-AZO can be reduced and yield aniline derivative.[19] Therefore, Cas9/sgRNA ribonucleoprotein complex was released from AuNRs to specifically knock out HSP90α gene, which greatly reduced the thermal tolerance of tumor cells. In this way, a tumor-targeted mild therapeutic

[*] X. Li,[+] Y. Pan,[+] Dr. Y. Gao, Dr. X. Liu, X. Luan, D. Zhou, F. Zeng, Prof. Dr. Y. Song
College of Engineering and Applied Sciences, Jiangsu Key Laboratory of Artificial Functional Materials, State Key Laboratory of Analytical Chemistry for Life Science, Nanjing University
Nanjing 210023 (China)
E-mail: ysong@nju.edu.cn
C. Chen, Dr. K. Yang, Prof. Dr. X. Han
School of Medicine & Holistic Integrative Medicine, Jiangsu Collaborative Innovation Canter of Chinese Medicinal Resources Industrialization, Nanjing University of Chinese Medicine
Nanjing 210023 (China)
E-mail: xhan0220@njucm.edu.cn
[+] These authors contributed equally to this work.
Supporting information and the ORCID identification number(s) for the author(s) of this article can be found under: https://doi.org/10.1002/anie.202107036.

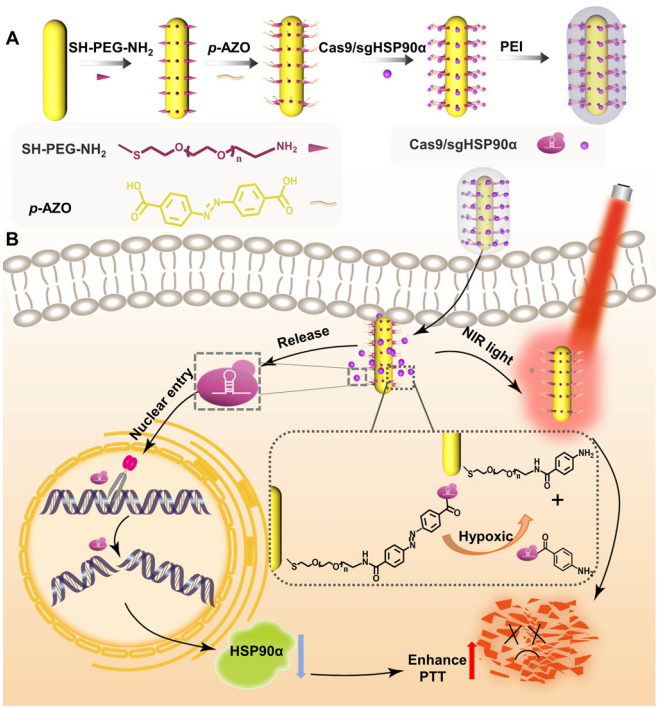

Figure 1. Design of the hypoxia-responsive CRISPR-Cas9 system to reduce tumor thermal tolerance. A) Preparation of APACPs. B) Hypoxia-triggered delivery of Cas9-sgHSP90α to the nucleus for gene editing and mild-photothermal therapy carried out with NIR light.

effect on deeper tissues was achieved upon NIR light (808 nm) irradiation with a relatively low power.

The tailored design of hypoxia-activated CRISPR-Cas9 nanosystem (APACPs) was displayed in Figure 1 A. As-synthesized AuNRs[20] were first treated with SH-PEG-NH_2 (denoted as APs) and then conjugated with the hypoxia-sensitive linker, azobenzene-4,4′-dicarboxylic acid (termed as APAs). Subsequently, Cas9/sgRNA ribonucleoprotein complexes were covalently assembled on the APAs by carbodiimide hydrochloride/N-hydroxysuccinimide coupling (denoted as APACs). To facilitate cell uptake, the resulting nanoparticles were wrapped by positively charged polyethylenimine (PEI), yielding APACPs with a modified organic layer including Cas9 of 2 nm (Figures 2 A, B, and S1). The stepwise modification process of preparing APACPs was also verified by zeta potential analysis and Fourier Transform Infrared Spectrometer (FT-IR) (Figure 2 C and F). For directly confirming the successful assembly of Cas9/sgRNA, high magnification TEM was monitored, and obvious gold and phosphorus elements were discovered in APACPs, corresponding to AuNRs and sgRNA, respectively (Figure 2 D). Moreover, UV-vis absorbance spectra showed that the longitudinal Surface Plasmon Resonance (SPR) peak of AuNRs appeared an 83 nm redshift from 688 nm of AuNRs to 771 nm after modification (Figure 2 E). Besides, the photothermal effect of APACPs was detected, and results demonstrated that the photothermal efficiency of APACPs was highly dependent on power density and concentration (Figures S2 and S3).

Subsequently, we evaluated the Cas9-binding capacity of our nanosystem by gel electrophoresis. As shown in Figures 3 B and S4, 1 μg of Cas9 could be substantially connected with 4.0×10^{-5} nmol of APs via carbodiimide cross-linker chemistry. Next, we explored the hypoxia-responsive Cas9 release in Tris-HCl. Here, sodium hydrosulfite (SDT) was employed as a analog of azoreductase, which could break the azo bond in our nanosystem.[18b] For convenience in analyzing, we labelled the Cas9 on AuNR nanocomplexes with cyanine3 (Cy3). Once the *p*-AZO was destroyed by SDT, the Cas9 was released from the AuNRs, leading to a significant fluorescent signal (Figure 3 A). As shown in Figure 3 C, enhanced fluorescence intensities were readily observed after SDT added, and such intensity was positively correlated with SDT concentration. Afterwards, the release of Cas9 over time in the presence of SDT was investigated. We discovered that the

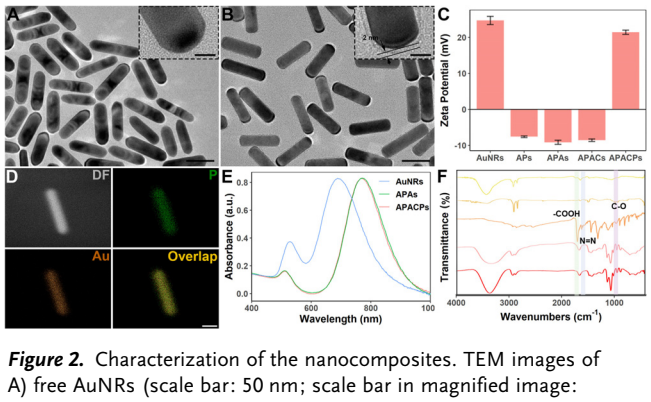

Figure 2. Characterization of the nanocomposites. TEM images of A) free AuNRs (scale bar: 50 nm; scale bar in magnified image: 10 nm), B) APACPs (scale bar: 50 nm; scale bar in magnified image: 10 nm), and D) its TEM mapping (scale bar: 25 nm). C) The zeta potential of AuNRs, APs, APAs, APACs, and APACPs. Bars represent mean ± SD ($n=3$). E) UV-vis absorbance spectra of AuNRs, APAs, and APACPs. F) FITR spectra of AuNRs, APs, APAs, APACs, and APACPs (from top to bottom).

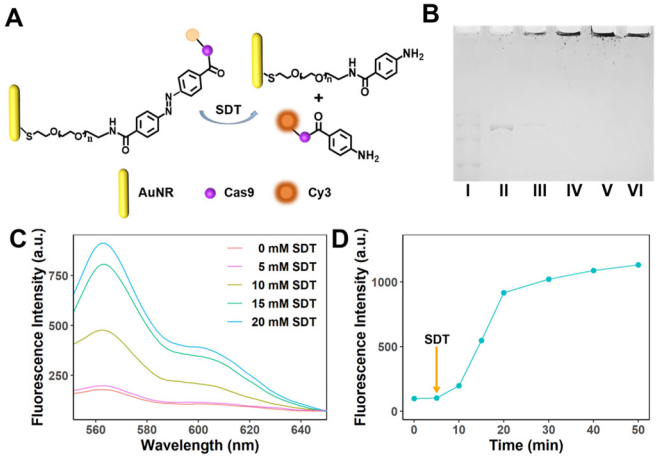

Figure 3. Verification of Cas9 connection and release. A) Schematic illustration of the release of Cas9 protein labeled by Cy3 from APACPs under simulated hypoxia by SDT. B) SDS-acrylamide gel electrophoresis of Cas9 and Cas9/APA complexes. I. Marker, II. 1 μg Cas9, III. 1 μg Cas9 + 4.0×10^{-6} nmol APAs, IV. 1 μg Cas9 + 4.0×10^{-5} nmol APAs, V. 1 μg Cas + 1.20×10^{-4} nmol APAs, VI. 1.20×10^{-4} nmol APs. C) Fluorescence spectra of Cas9 released from APACs at various SDT concentrations. D) The release of Cas9 over time under the action of SDT.

fluorescence intensity rapidly increased in 10 minutes (Figure 3D). Besides, liver microsomes under hypoxia environment were employed to further investigate the controllable releasing of Cas9, and the similar results were obtained as shown in Figure S5. These results demonstrated the efficient hypoxia-responsive release of Cas9 protein, which constituted a desirable property for tumor-targeted gene editing and precision medicine.

To test the cytotoxicity of the nanoparticles, A549 cells (a human lung adenocarcinoma cell line) were treated with APACPs at different doses (0, 0.05, 0.1, 0.2, 0.4 nM). After 48 hours, the viability of cells was evaluated by the Cell Counting Kit-8 (CCK-8) assay. As shown in Figure 4A, no

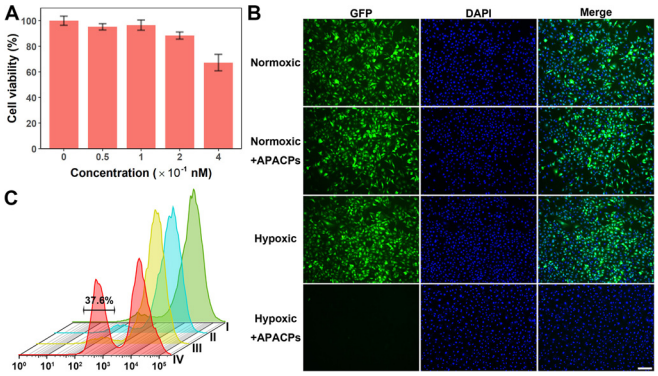

Figure 4. Hypoxia-responsive release of Cas9 for gene editing. A) Relative viabilities of A549 cells incubated with APACPs of different doses. B) Fluorescence microscopy images (scale bar: 100 μm) and C) flow cytometry analysis of A549-EGFP cells subjected to the following conditions: I. normoxic, II. normoxic + APACPs, III. hypoxic, IV. hypoxic + APACPs.

measurable cytotoxicity was observed at concentrations below 0.2 nM, whereas higher concentrations (0.4 nM) led to a decreased cell viability (about 67%) compared with untreated cells. Thus, the concentration of 0.1 nM of APACPs was adopted in the subsequent experiments. Next, the intracellular hypoxia response of our system was detected by incubation of Cy3-labelled APACPs with modified A549 cells that express enhanced green fluorescent protein stably (A549-EGFP cells). Since the azobenzene group could be cleaved by the increased expression of reductive species in hypoxia environment (< 1% O_2), the Cas9 ribonucleoprotein complexes could be released from AuNRs and entered nucleus for gene editing. Evidence of the hypoxia-triggered character releasing was demonstrated by confocal laser scanning microscopy (CLSM). Significant Cy3 fluorescent signals were observed in the nucleus under hypoxic conditions, while the APACPs were blocked by nuclear membrane and negligible red fluorescence was observed in the nucleus under normoxic condition after 8-hour treatment (Figure S6).

Subsequently, we investigated the hypoxia-triggered gene editing in vitro. An A549-EGFP cell and EGFP-targeting sgRNA (sgEGFP) were applied to assess the editing efficiency here. After culturing for 48 hours, a dramatic decrease in green channel was observed in the hypoxic cells treated with APACPs, while other groups demonstrated no observable change (Figure 4B). The EGFP-negative cells were quantified by flow cytometry analysis. Results indicated that approximately 37.6% of the A549-EGFP cells incubated with APACPs under hypoxia condition displayed EGFP knockout, whereas the EGFP-negative cells in other methods could be ignored (Figure 4C). Both the fluorescence microscopy and flow cytometry indicated the effectiveness of APACPs in vitro gene editing under hypoxic conditions. It was confirmed that the on-demand release of Cas9 could achieve to edit the target gene effectively.

After demonstrating the targeted gene editing, we studied the prohibitory effect of APACPs on tumor cell proliferation. The HSP90α gene was chosen as the target locus here to be knocked out for anticancer under low-temperature hyperthermia (Figure 5A). We first screened appropriate gene site by T7E1 experiments. As shown in Figure S7, T7EI enzyme could effectively cut the target sequence into two bands of 196 bp and 352 bp in size in the group of sgRNA sequence 2, and thereby sgRNA sequence 2 was selected to guide the Cas9 for HSP90α gene editing in subsequent experiments. Next, we cultured A549 cells with various treatments, i.e., group 1: normoxia, group 2: normoxia plus APACPs, group 3: hypoxia, group 4: hypoxia plus APACPs. As expected, the cell death rate of A549 cells co-treated with APACPs plus NIR light irradiation in hypoxia increased significantly to 52.0%, which was much higher than that of the cells treated by other methods (Figure 5D and E), suggesting an enhanced cell killing effect via the combination of PTT and hypoxia-activated Cas9. The cell viability measured by CCK-8 assay and fluorescent microscope also confirmed the above results (Figure S8). To further verify the synergetic effect, A549 cells were, respectively treated with AuNRs and APACPs under NIR irradiation with different power densities (0.75, 1.5,

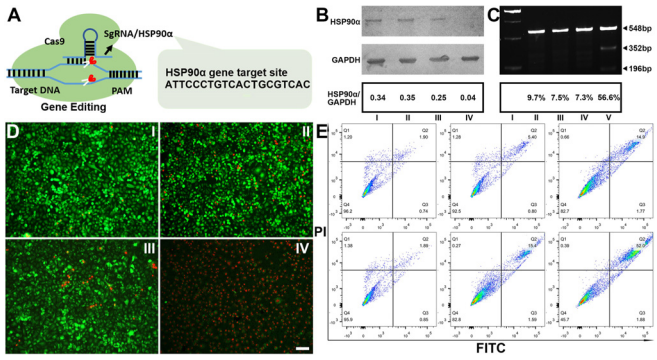

Figure 5. The cooperation of NIR irradiation and gene editing caused apoptosis of A549 cells. A) Schematic diagram of Cas9/sgHSP90α gene editing. B) Western blot analysis of the HSP90α protein expression in A549 cells treated with or without APACPs nanoparticles under normoxic or hypoxic conditions: I. Normoxia, II. normoxia + APACPs, III. hypoxia, IV. hypoxia + APACPs. C) Surveyor assay for indel frequency analysis of A549 cells incubated with or without APACPs nanoparticles under normoxic or hypoxic conditions: I. normoxia, II. normoxia + APACPs, III. hypoxia, IV. hypoxia + APACPs. D) Fluorescence images of cells treated by I. APACPs, II. APACPs + NIR, III. APACPs + hypoxia, IV. APACPs + hypoxia + NIR. Green: calcein-AM; red,:PI. Scale bar: 100 μm. E) Flow cytometry assay of cell apoptosis with indicated treatments.

2.25 W cm^{-2}). As damages from low temperature could be repaired by cancer cells with the assistant of HSP, the AuNRs hardly induced a complete cell necrosis. In contrast, HSP90 knockout by Cas9 reduced thermoresistance of A549 cells, and hence the cytotoxicity of APACPs increased significantly with the increase of power density (Figure S9).

For gaining insight into the mechanism of the Cas9-mediated mild PTT, we directly cultured cells in different temperatures. As shown in Figure S10, the cells were killed at 50 °C but lived well at 37 °C, while the cells treated with APACPs had a higher rate of apoptosis compared to the cells treated with AuNRs at 42 °C. Following western blot demonstrated that co-treatment of the nanoparticles and hypoxia dramatically led to a down-regulation of HSP90α compared with other treatments (Figure 5B). To assess whether the decrease in protein was originated from the formation of indel, we evaluated gene editing efficiency by SURVEYOR and high-throughput sequence assay. The gene-editing efficiency induced by APACPs treatment under hypoxic conditions was much higher than that in the control groups (Figures 5C, and S11). These results indicated that APACPs could achieve Cas9 releasing under hypoxic conditions and knockout out the HSP90α gene for suppressing thermoresistance of cancer cells, enabling effective available therapy at lower irradiation.

Next, we studied the antitumor effect of APACPs in vivo (Figure 6A). The A549 tumor-bearing nude mice were intravenously (i.v.) injected with Cy5-labled APACPs first to evaluate the tumor retention of APACPs. We recorded the biodistribution of APACPs via an animal imaging system at various time points. As shown in Figure S12, the fluorescence signals in heart, spleen, and lung can be readily observed at 12 hours, and dramatically decreased after 48 hours, indicating that most of injected nanoparticles could be excreted out from body. Conversely, APACPs would accumulate at tumor site, and the fluorescence signals still maintained a high level after 48-hour injection (Figure S12). Subsequently, we randomly divided a total of 20 nude mice bearing A549 tumors into 4 groups: 1) PBS (control); 2) APACPs; 3) AuNRs + NIR; 4) APACPs + NIR, and recorded the tumor sizes of different groups in 20 days (Figure 6B). Obviously, compared with other treatment methods, APACPs + NIR could significantly inhibit the growth of tumor. On day 21, all mice were sacrificed and the tumors were collected, photographed, and weighed to further confirm the amplified antitumor efficacy (Figure 6C and D). Moreover, as revealed by Hematoxylin and eosin (H&E) staining, in situ TUNEL assay, and KI67 staining, the most severe damage to tumor was observed in group 4, whereas lower levels of hurt were detected in the control groups (Figure S13). In addition, the immunohistochemical study of HSP90α at tumor sites was performed. The decreased HSP90α expression was found in group 2, and 4, while negligible suppressing effect in the other groups was obtained (Figure S14), which strongly evidence that APACPs could lead to an available thermoresistance reducing of cancer cells via the Cas9-mediated HSP90α knockout for mild PTT. The similar results were also found by mutation analysis (Figures 6E, F, and S15). The editing efficiency of group 2 is slightly higher than that of group 4, which probably resulted from temperature effect on enzyme activity. To further demonstrate the hypoxia-response gene editing via systemic injection for sure, the Polo-like Kinase 1 (PLK-1) gene which is associated with cancer cell proliferation was chosen as target site for Cas9. Compared with the nanoparticles (APCPs-PLK-1) without hypoxia-responsive azobenzene group, the intravenous administration of APACPs in which Cas9-sgRNA targeted PLK-1(APACPs-PLK-1) displayed an obvious suppressive effect on tumor development (Figure S16), which confirmed the hypoxia response performance of our design. Meanwhile, the APACP nanoparticles treatment had no effect on the body weight of mice (Figure S17), and no significant damage to the organ slices was observed in the experimental group (Figure S18), indicating the biological safety of this method.

Finally, we investigated the anticancer effect of APACPs against orthotopic lung tumor. Compared with the subcutaneous transplantation model, orthotopic tumor model built a more realistic tumor microenvironment and possessed a higher clinical relevance. Here, to monitor the tumor growth, micro-CT was employed and the results were revealed as shown in Figure S19C, where the mice treated with APACPs and NIR irradiation demonstrated weaker changes than that of other groups throughout the 18 day therapeutic course. The number of tumor nodules in the lungs after 18 day treatment was significantly inhibited in the APACPs + NIR group (Figure S19D). And the group maintained well-organized lung tissue, while widespread damage of alveolar structure was observed in other groups (Figure S19E). In addition, body weights of the mice treated with

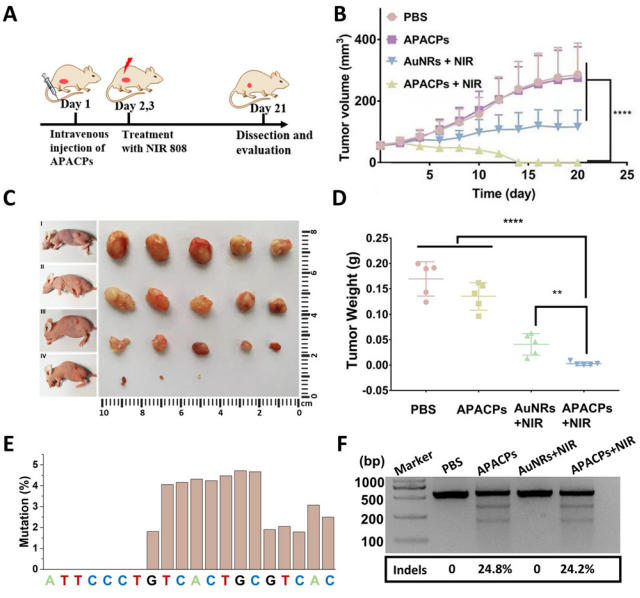

Figure 6. The antitumor effect of APACPs in vivo. A) Schematic of nude mice treatment. B) Tumor volume after different methods as indicated. C) Images of tumors treated by I. PBS, II. APACPs, III. AuNRs + NIR, IV. APACPs + NIR. D) Weights of tumors treated by different methods. E) Mutation rate profiles for HSP90α in tumor after treatment with APACPs. F) Surveyor assay for indel frequency analysis of tumors with indicated treatment. $^{**}p < 0.01$ represents significant difference and $^{****}p < 0.0001$ represents highly significant difference.

APACPs + NIR exhibited slight increase in the 18 days, further demonstrating the high efficacy of APACPs (Figure S19B).

In summary, we constructed a hypoxia-responsive nanosystem for Cas9-mediated mild PTT. In the system, a hypoxia-responsive azobenzene was employed to covalently bridge CRISPR system and AuNRs. By preparing a single guide RNA targeting HSP90α, AuNRs were applied to a photothermal converter that transformed NIR light (808 nm) into intracellular heat to achieve targeted mild hyperthermia and synergistic anticancer effects both in vitro and in vivo. This gene editing-based nanosystem effectively overcame hyperthermia-induced heating damage of healthy organs nearby and killed cancer cells in a minimally invasive manner, which hold enormous potential for future clinical translation. More importantly, such work presents an elegant strategy for tumor-targeted gene editing and bridged CRISPR-Cas9 technology for precision medicine.

Acknowledgements

We acknowledge the National Key R&D Program of China (2019YFA0709200), the financial support from the National Natural Science Foundation of China (21874066, 81601632, and 31901010), the Fundamental Research Funds for Central Universities, the Natural Science Foundation of Jiangsu Province (BK20160616 and BK20200336), the Program for Innovative Talents and Entrepreneur in Jiangsu, Jiangsu Specially Appointed Professorship Foundation, and Postgraduate Research & Practice Innovation Program of Jiangsu Province (KYCX20_0036).

Conflict of Interest

The authors declare no conflict of interest.

Keywords: antitumor agents · CRISPR/Cas9 · gene editing · photothermal therapy · targeted delivery

[1] a) J. Travis, *Science* **2015**, *350*, 1456 – 1457; b) P. D. Hsu, E. S. Lander, F. Zhang, *Cell* **2014**, *157*, 1262 – 1278; c) J. A. Doudna, E. Charpentier, *Science* **2014**, *346*, 1258096; d) H. Chen, S. Bailey, *Science* **2016**, *351*, 811 – 812.

[2] a) L. Zhang, L. Wang, Y. Xie, P. Wang, S. Deng, A. Qin, J. Zhang, X. Yu, W. Zheng, X. Jiang, *Angew. Chem. Int. Ed.* **2019**, *58*, 12404 – 12408; *Angew. Chem.* **2019**, *131*, 12534 – 12538; b) W. Sun, W. Ji, J. M. Hall, Q. Hu, C. Wang, C. L. Beisel, Z. Gu, *Angew. Chem. Int. Ed.* **2015**, *54*, 12029 – 12033; *Angew. Chem.* **2015**, *127*, 12197 – 12201; c) H. Park, J. Oh, G. Shim, B. Cho, Y. Chang, S. Kim, S. Baek, H. Kim, J. Shin, H. Choi, J. Yoo, J. Kim, W. Jun, M. Lee, C. J. Lengner, Y. K. Oh, J. Kim, *Nat. Neurosci.* **2019**, *22*, 524 – 528; d) Y. Nihongaki, T. Otabe, M. Sato, *Anal. Chem.* **2018**, *90*, 429 – 439.

[3] D. J. Wells, *Gene Ther.* **2004**, *11*, 1363 – 1369.

[4] R. Maurisse, D. De Semir, H. Emamekhoo, B. Bedayat, A. Abdolmohammadi, H. Parsi, D. C. Gruenert, *BMC Biotechnol.* **2010**, *10*, 9.

[5] Y. Zhang, H. Li, Y. L. Min, E. Sanchez-Ortiz, J. Huang, A. A. Mireault, J. M. Shelton, J. Kim, P. P. A. Mammen, R. Bassel-Duby, E. N. Olson, *Sci. Adv.* **2020**, *6*, eaay6812.

[6] a) P. Wang, L. Zhang, W. Zheng, L. Cong, Z. Guo, Y. Xie, L. Wang, R. Tang, Q. Feng, Y. Hamada, K. Gonda, Z. Hu, X. Wu, X. Jiang, *Angew. Chem. Int. Ed.* **2018**, *57*, 1491 – 1496; *Angew. Chem.* **2018**, *130*, 1507 – 1512; b) H. X. Wang, Z. Song, Y. H. Lao, X. Xu, J. Gong, D. Cheng, S. Chakraborty, J. S. Park, M. Li, D. Huang, L. Yin, J. Cheng, K. W. Leong, *Proc. Natl. Acad. Sci. USA* **2018**, *115*, 4903 – 4908; c) Y. Pan, J. Yang, X. Luan, X. Liu, X. Li, J. Yang, T. Huang, L. Sun, Y. Wang, Y. Lin, Y. Song, *Sci. Adv.* **2019**, *5*, eaav7199; d) J. B. Miller, S. Zhang, P. Kos, H. Xiong, K. Zhou, S. S. Perelman, H. Zhu, D. J. Siegwart, *Angew. Chem. Int. Ed.* **2017**, *56*, 1059 – 1063; *Angew. Chem.* **2017**, *129*, 1079 – 1083.

[7] a) C. Li, R. J. Samulski, *Nat. Rev. Genet.* **2020**, *21*, 255 – 272; b) M. A. Kotterman, D. V. Schaffer, *Nat. Rev. Genet.* **2014**, *15*, 445 – 451.

[8] a) T. Wei, Q. Cheng, L. Farbiak, D. G. Anderson, R. Langer, D. J. Siegwart, *ACS Nano* **2020**, *14*, 9243 – 9262; b) H. X. Wang, M. Li, C. M. Lee, S. Chakraborty, H. W. Kim, G. Bao, K. W. Leong, *Chem. Rev.* **2017**, *117*, 9874 – 9906.

[9] R. A. Gatenby, R. J. Gillies, *Nat. Rev. Cancer* **2008**, *8*, 56 – 61.

[10] N. C. Denko, *Nat. Rev. Cancer* **2008**, *8*, 705 – 713.

[11] a) A. J. Primeau, A. Rendon, D. Hedley, L. Lilge, I. F. Tannock, *Clin. Cancer Res.* **2005**, *11*, 8782 – 8788; b) L. Harrison, K. Blackwell, *Oncologist* **2004**, *9 Suppl 5*, 31 – 40.

[12] J. N. Liu, W. Bu, J. Shi, *Chem. Rev.* **2017**, *117*, 6160 – 6224.

[13] L. Song, X. Zhou, X. Dai, R. Wang, G. Cheng, N. Zhao, F.-J. Xu, *NPG Asia Mater.* **2018**, *10*, 509 – 521.

[14] G. Gao, Y. W. Jiang, W. Sun, Y. Guo, H. R. Jia, X. W. Yu, G. Y. Pan, F. G. Wu, *Small* **2019**, *15*, 1900501.

[15] a) C. W. Song, H. Park, R. J. Griffin, *Radiat. Res.* **2001**, *155*, 515 – 528; b) H. Luo, Q. Wang, Y. Deng, T. Yang, H. Ke, H. Yang, H. He, Z. Guo, D. Yu, H. Wu, H. Chen, *Adv. Funct. Mater.* **2017**, *27*, 1702834.

[16] a) L. Whitesell, S. L. Lindquist, *Nat. Rev. Cancer* **2005**, *5*, 761 – 772; b) J. Trepel, M. Mollapour, G. Giaccone, L. Neckers, *Nat. Rev. Cancer* **2010**, *10*, 537 – 549.

[17] a) A. Subbarao Sreedhar, É. Kalmár, P. Csermely, Y.-F. Shen, *FEBS Lett.* **2004**, *562*, 11 – 15; b) M. Zou, A. Bhatia, H. Dong, P. Jayaprakash, J. Guo, D. Sahu, Y. Hou, F. Tsen, C. Tong, K. O'Brien, A. J. Situ, T. Schmidt, M. Chen, Q. Ying, T. S. Ulmer, D. T. Woodley, W. Li, *Oncogene* **2017**, *36*, 2160 – 2171.

[18] a) S. Kizaka-Kondoh, M. Inoue, H. Harada, M. Hiraoka, *Cancer Sci.* **2003**, *94*, 1021 – 1028; b) W. C. Geng, S. Jia, Z. Zheng, Z. Li, D. Ding, D. S. Guo, *Angew. Chem. Int. Ed.* **2019**, *58*, 2377 – 2381; *Angew. Chem.* **2019**, *131*, 2399 – 2403.

[19] a) F. Zhou, T. Fu, Q. Huang, H. Kuai, L. Mo, H. Liu, Q. Wang, Y. Peng, D. Han, Z. Zhao, X. Fang, W. Tan, *J. Am. Chem. Soc.* **2019**, *141*, 18421 – 18427; b) G. Yang, S. Z. F. Phua, W. Q. Lim, R. Zhang, L. Feng, G. Liu, H. Wu, A. K. Bindra, D. Jana, Z. Liu, Y. Zhao, *Adv. Mater.* **2019**, *31*, 1901513; c) W. Piao, S. Tsuda, Y. Tanaka, S. Maeda, F. Liu, S. Takahashi, Y. Kushida, T. Komatsu, T. Ueno, T. Terai, T. Nakazawa, M. Uchiyama, K. Morokuma, T. Nagano, K. Hanaoka, *Angew. Chem. Int. Ed.* **2013**, *52*, 13028 – 13032; *Angew. Chem.* **2013**, *125*, 13266 – 13270; d) C. Huang, J. Zheng, D. Ma, N. Liu, C. Zhu, J. Li, R. Yang, *J. Mater. Chem. B* **2018**, *6*, 6424 – 6430.

[20] a) X. Zhao, C. X. Yang, L. G. Chen, X. P. Yan, *Nat. Commun.* **2017**, *8*, 14998; b) J. H. Wang, B. Wang, Q. Liu, Q. Li, H. Huang, L. Song, T. Y. Sun, H. Wang, X. F. Yu, C. Li, P. K. Chu, *Biomaterials* **2013**, *34*, 4274 – 4283.

Manuscript received: May 26, 2021
Accepted manuscript online: July 23, 2021
Version of record online: August 17, 2021

